

## **General Disclaimer**

### **One or more of the Following Statements may affect this Document**

- This document has been reproduced from the best copy furnished by the organizational source. It is being released in the interest of making available as much information as possible.
- This document may contain data, which exceeds the sheet parameters. It was furnished in this condition by the organizational source and is the best copy available.
- This document may contain tone-on-tone or color graphs, charts and/or pictures, which have been reproduced in black and white.
- This document is paginated as submitted by the original source.
- Portions of this document are not fully legible due to the historical nature of some of the material. However, it is the best reproduction available from the original submission.

092307

MAGNETIC DIPS IN THE SOLAR WIND

M.Dobrowolny, B.Bavassano, F.Mariani,  
N.Ness and L.Burlaga

LPS-78-7

September 1978

RECEIVED BY

ESA - SDS

DATE:

25 GEN. 1979

DCAF NO.

320100

PROCESSED BY

NASA STI FACILITY

ESA - SDS  AMR

LABORATORIO DI RICERCA E TECNOLOGIA  
PER LO STUDIO DEL PLASMA NELLO SPAZIO

CONSIGLIO NAZIONALE DELLE RICERCHE

VIA G. GALILEI - FRASCATI

MAGNETIC DIPS IN THE SOLAR WIND

M.Dobrowolny, B.Bavassano, F.Mariani

Laboratorio Plasma Spazio, CNR, Frascati, Italy

N.Ness and L.Burlaga

Laboratory for Extraterrestrial Physics,  
NASA/Goddard Space Flight Center,  
Greenbelt, Md., U.S.A.

## ABSTRACT

Using magnetic data from the HELIOS 1 fluxgate magnetometer, with a 0.2 s resolution, we have investigated the structure of several interplanetary discontinuities involving magnetic dips and rotations of the magnetic field vector. A minimum variance analysis illustrates the behaviour of the magnetic field through the transition in the plane of its maximum variation. Using this analysis, quite different structures have been individuated and, in particular, narrow transitions resembling almost one dimensional reconnected neutral sheets. For the thinner cases (scale lengths of the magnetic rotation of the order or smaller than  $10^3$  km), we find that the observed structures can be the non linear effect of a resistive tearing mode instability having developed on an originally one dimensional neutral sheet at the solar corona.

## 1. INTRODUCTION.

The nature of the discontinuities shown by magnetic data in the solar wind, has been the subject of several studies and controversies (Burlaga, 1971a).

In general, most of these studies have been centered on the problem of identifying such discontinuous transitions in terms of a magnetohydrodynamic classification, i.e. as tangential or rotational discontinuities (Siscoe et al., 1968; Burlaga 1971a; Martin et al., 1973; Mariani et al., 1973).

Correspondingly, in most of such previous studies, owing also to the resolution of the experimental data, the actual structure of these boundary layers has not been looked in detail.

Only more recently, higher resolution magnetic data from the Explorer 43 spacecraft, have allowed investigations of the inner structure of such magnetic transitions (Burlaga et al., 1976; Turner et al., 1976).

We must notice that, when one wants to discuss, in physical terms, the inner structure of discontinuities, the very notion of discontinuity is in fact lost and one has to abandon the simple magnetohydrodynamic description and resort to more sophisticated plasma dynamic processes. This has to be kept in mind even if, in the following, we will sometimes still use the word discontinuity for the events considered.

On the other hand, as will be seen in the following, the analysis of the structure of discontinuities may be of great interest, in that these transitions may be the seat of interesting plasma processes, which can then be isolated and studied.

This paper presents an analysis of several small scale magnetic transitions (or interplanetary discontinuities), where the

0.2 second resolution data of the Rome-Goddard magnetic experiment on board of HELIOS 1, have been used.

More specifically, the magnetic transitions which we have chosen to study are characterized by magnetic dips, i.e. quite strong depressions of the magnetic field magnitude, with respect to the average interplanetary value, and simultaneous rotations of the magnetic field vector.

A number of structures with the above qualitative features, have been put into evidence, among tangential discontinuities, quite a long time ago by Burlaga and Ness (1969) and given the name D sheets. The examples reported by Burlaga and Ness

, where taken from Pioneer 6 data at much lower resolution than that of the present HELIOS data.

A main reason of interest in these magnetic dips, lies in the possibility that detailed studies of them may give evidence of some process of magnetic reconnection, having occurred or taking place. In turn, a clear understanding of magnetic reconnection processes is of fundamental importance in many astrophysical situations and, in particular, in the physics of planetary magnetospheres.

The idea that magnetic dips in the solar wind may have something to do with magnetic reconnection, was advanced by Burlaga and Ness (1969), in relation to the D sheets previously mentioned. That idea, which we will discuss later on, was however purely based on geometrical arguments and not supported by a discussion of possible underlying physical processes.

More recently, Burlaga and Scudder (1974) have tried to compare the Pioneer 6 D sheet data with the Sweet's model of steady state magnetic reconnection (Sweet, 1967; Parker, 1968) and have given some evidence that the observed profiles of magnetic field and pressure, are consistent with the analytical predictions of

such model.

The scheme of our paper is the following: in Sect. 2 we show, from HELIOS 1 data, some selected cases of magnetic dips in the solar wind and discuss the results of a minimum variance analysis, performed on such cases. The features of the events analyzed are also compared with those of the D sheets of the previous literature, and with other small scale magnetic structures, called "magnetic holes", which were recently reported (Turner et al., 1976). Using also the plasma velocities from the plasma experiment on HELIOS 1 (Rosenbauer et al., 1977), we determine the thickness of the current sheets involved.

Sect. 3 illustrates some theoretical ideas on the origin and physical nature of such magnetic dips. In Sect. 4, using both magnetic and plasma data, we test, more specifically, the theoretical hypothesis that, at least some of the events observed, are the non linear effect of the development of a tearing mode instability (Furth et al., 1964; Dobrowolny, 1968), leading to magnetic line reconnection from an original configuration resembling an ideal neutral sheet.

In Sect. 5 we discuss the results obtained. In particular, we comment on the degree of evidence which has been reached for the occurrence of tearing modes, and we point out further work (based also on the consideration of high resolution plasma data), which is necessary to obtain more definite conclusions on the occurrence of a reconnection process, either the tearing instability or some form of steady state reconnection.

## 2. OBSERVATIONS OF MAGNETIC DIPS IN THE SOLAR WIND.

HELIOS 1 was launched on December 10, 1974 into solar elliptic orbit with a period of 190 days, an aphelion of 0.98 AU and a perihelion of .31 AU. The spacecraft is spin stabilized with the spin axis perpendicular to the ecliptic plane and a spin period of 1 s.

The Rome-GSFC magnetic field experiment on board of HELIOS 1 consists of a triaxial fluxgate magnetometer with four automatically switchable measurement ranges. The sampling rate depends upon the telemetry format and bit rate. For the selected events the sampling time interval is 187.5 ms, except for one case, day 85, when this interval is 1.5 s. Further informations about the experiment are given by Searce et al. (1975).

The events which are analyzed in this paper are listed in Table 1. The first column there gives their approximate time localization and the second column the distance from the Sun. Remaining quantities on the Table will be commented later on.

Figs. 1-3 are plots of the magnetic variations, as seen in solar ecliptic coordinates, for some of the events considered day 18, 122 and 44.

Within the available data, the events were chosen with the general criterium of having well pronounced magnetic dips and clearly associated rotations of the magnetic field vector, with possibly no or little superposition of strong fluctuations.

A second criterium of choice was that of having both events where the magnetic rotation appears to be sharply localized with respect to the duration of the magnetic dip (cases of day 22, 26, 85, see also Fig. 2) and cases (day 3, 85, see also Fig. 1) where the magnetic rotation appears more gradual. The event of day



44 (see Fig. 3) is unique among the others considered in that, as can be seen from Fig. 3 both the magnetic dip and the associated rotation are extremely sharp occurring in only  $\sim 0.5$  seconds.

Finally, it should be remarked that, although the  $\phi$  rotation amounts, in all cases, to about  $180^\circ$  (see Figs. 1-3), the events chosen are not sector boundaries. The angular state reached after the magnetic transition does not, in fact, last for a long time, as could be seen by looking at data plots over longer periods. The situation, as far as sector boundaries are concerned, measured by KILLIOS 1 is discussed in a very recent paper by Mariani et al. (1978).

Some comments are in order on the relation of the events considered with other discontinuities characterized by magnetic depressions, which have been reported in the literature.

A first point is that these events appear to be something different from the so called "magnetic holes" reported recently by Turner et al. (1977). In such magnetic holes, the depression of magnetic field was either not accompanied by any rotation (unlike any of the cases presented here), or, in case of a simultaneous rotation, the rotation was gradual along the dip. Although this appears to be similar to our events of days 3 and 85 (see also Fig. 1), the duration of the holes, reported by Turner et al. (1977), was much smaller, of the order of 10 seconds, than the duration of our magnetic dips (of the order of 1 minute or more, for day 3 and 85).

Our events of day 22 and 26 (see Fig. 1) could be taken as similar to the D sheets reported early by Burlaga and Ness (1969), in that the magnetic rotation appears there very sharp in comparison with the duration of the dip. In contrast, however, these two events have a duration of the magnetic depression, of the order or smal-

ler than one minute, much shorter than that of the Pioneer 6 D sheets, which appeared to be about one order of magnitude longer.

Finally, the extremely sharp event of Fig. 3 cannot be compared with anything previously appeared in the literature. The rotations of the magnetic field in the events considered are indicative of the reversal of a magnetic field component. To obtain a useful representation of the magnetic field variations, we have performed a minimum variance analysis by using a technique first applied by Sonnerup and Cahill (1967). The variance matrix, defined by

$$S_{ij} = \langle B_i B_j \rangle - \langle B_i \rangle \langle B_j \rangle \quad (1)$$

where  $i$  and  $j$  refer to the solar ecliptic components of the magnetic field  $B$  and the angle brackets denote averaging over a specified time interval, has been diagonalized yielding the eigenvalues  $E_1 \geq E_2 \geq E_3$  and the corresponding eigenvectors  $\underline{V}_1, \underline{V}_2, \underline{V}_3$  which form the principal axes of the variance ellipsoid.

For each of the events considered, we have thus determined a direction ( $\underline{V}_3$ ) of minimum variation (i.e. a direction associated with an almost constant magnetic field component) and, correspondingly, a plane ( $\underline{V}_1 - \underline{V}_2$ ), normal to this direction, which we can call the plane of maximum magnetic field variation.

Table 2 shows the properties of the eigenvalues and the eigenvectors referring to the events indicated. Here  $x, y, z$  are the eigenvector components referring to solar ecliptic coordinates. In the column of Table 2 labelled  $(\Delta t)$ , we have indicated the interval of time, where the minimum variance analysis (giving the results reported in the Table), has been applied. This interval has been chosen so as to embrace the  $\phi$  rotation of the magnetic

field. Finally, in the column labelled N, we have listed the number of magnetic measurements taken in each variance analysis. As seen from Table 2, in each case, the eigenvalue  $E_3$  is much smaller than the other two, so that it is indeed found that the magnetic field variation takes place essentially in a plane. The orientation of such plane, where the magnetic rotation occurs, appears however to be different in the various cases, and no regularity in the orientation of such plane seems to be indicated. Clearly, however, an attempt to search for some preferential orientation of these magnetic sheets, would necessarily involve the analysis of many more events.

Figs. 4-6 represent, for the events shown in Figs. 1-3 respectively, the variations of the magnetic field components with respect to the axes ( $V_1$ ,  $V_2$ ,  $V_3$ ) of the minimum variance ellipsoid. If we look at the component ( $V_3$ ) in the direction of minimum variation, we find that this is essentially zero, in the case of Fig. 5, which therefore represents, in magnetohydrodynamic language, a tangential discontinuity. This is not quite so for the events of Fig. 4 and 6. Looking on the other hand at the components ( $V_1$ ,  $V_2$ ) in the plane of maximum variation, Fig. 5 shows also a quite peculiar feature, which is worthed to point out as it will be taken up in the theoretical discussion of Sect. 4.

The  $V_2$  component is approximately zero before the inversion but, at the inversion point, it becomes significantly different from zero, and, in fact, it is about  $0.5\gamma$  (which is above our uncertainties due to magnetic fluctuations and other causes, estimated of the order of  $0.1 \div 0.2 \gamma$ 's). We will call the  $V_2$  component, present at the zero of the  $V_1$  component, "a reconnecting" magnetic field component.

A similar, peculiar magnetic variation, with a substructure around

the magnetic reversal, inside the magnetic dip, is also obtained for the event of day 26 in Table 1. Notice also that such peculiar magnetic variations can be put into evidence only because of the very high data resolution and could not have been resolved (even if present) for events like the Pioneer 6 D sheets of Burlaga and Ness (1969).

Fig. 7 represents the successive change of orientation of the magnetic field vector in the plane of maximum variation, for all the 6 events listed in Table 1. More precisely, each of these diagrams is obtained by plotting consecutively (one for each measurement), in a given scale (which is indicated), the magnetic field vectors in the plane of maximum variation, each vector having its origin on the tip of the preceding vector, in temporal sequence. The point A, in each diagram, corresponds to the origin of the first magnetic vector and the point B to the tip of the last magnetic vector in the time interval indicated in each frame. This type of representation of the magnetic field rotation has been chosen, in place of a more usual hodograph representation, because of its conveniency in cases (like those of days 22, 26, 44) where in most of the transition the magnetic field direction is nearly the same and only the magnitude varies.

In this representation (see Fig. 7), we appreciate clearly some differences between the events chosen, which we think may have a physical significance (see Sect. 4). More specifically, from the plots of days 22, 26 and 44, in Fig. 7, we see that, in the intervals chosen for the minimum variance, it is essentially only one magnetic component ( $V_1$ ), which varies (the  $V_2$  component being negligible or much smaller) and, in a re-

stricted interval of time, where the  $V_1$  component has become very small, this almost one dimensional magnetic field configuration acquires a transverse component which connects the two antiparallel  $V_1$  components. This holds true, as can be seen in Fig. 7, also in the very restricted interval ( $\approx 0.5^\circ$ ) where the rotation of day 44 takes place (the minimum variance analysis there refers to a much larger interval in order to have a sufficient number of points). Thus, we have the right to say that the events of day 22, 26 and 44 are essentially one-dimensional "reconnected" neutral sheets.

In contrast, we cannot certainly call one-dimensional-reconnected neutral sheets the events of days 3, 18 and 85, where in fact we have always a quite large transverse ( $V_2$ ) component present, during all the magnetic depression.

In summary, the main conclusion of this minimum variance analysis, is that we may separate, among our magnetic dips, some which resemble almost one-dimensional neutral sheets (with however, a small, but non zero, transverse component at the point of inversion), from others where one has, during all the rotation, an essentially two-dimensional magnetic field variation.

### 3. COMMENTS ON THE ORIGIN AND PHYSICAL NATURE OF THE OBSERVED STRUCTURES.

We attempt in this section a discussion of possible theoretical ideas which can be relevant to understand small scale magnetic structures of the type previously shown.

Concerning, first of all, the origin of these structures and, more in general, of magnetic field tangential discontinuities in the solar wind, it must be said that no clear conclusions have been obtained from the previous works, mostly of a statistical nature, which have been quoted in Sect. 1. A tentative hypothesis of local generation of interplanetary field discontinuities, through the "impacts" of fast plasma streams with lower speed plasma, near 1 AU, has been ruled out by the appropriate data analysis (Burlaga, 1971).

More useful indications on the origin and nature of discontinuities, would come from studies of their rate of occurrence or, even more significantly, of their thickness as a function of distance from the Sun. Something of this type has indeed been reported (Tsurutani and Smith, 1975) from Pioneer 10 data, with the indication of an increasing thickness with increasing distance from the Sun. More systematic informations will certainly come from the analysis of Mariner 10 and the HELIOS spacecraft data.

It seems to us that, concerning in particular the type of discontinuities we have examined here, implying also magnetic field reversals, a most reasonable hypothesis is that of generation from magnetic structures in the inner corona, which are then convected far away in the solar wind flow.

As it is well known, the magnetic topology of the solar corona is characterized by regions of closed magnetic lines, as well as regions of open lines along which the coronal expansion takes place

preferentially.

The interface between regions of closed loops and those of open field lines, implies the formation of a neutral point and, at higher altitudes, a neutral sheet, i.e. and ideally thin region separating areas of opposite magnetic field polarity. Pneumann (1972) has developed a model of the successive evolution of such magnetic field topologies in the solar wind. Taking into account the effects of small (but finite) resistivity (which causes diffusion of plasma across magnetic lines), this theory predicts the possibility of having enormously distended magnetic tongues in the solar wind. Regions of magnetic field reversal, or abrupt changes of magnetic field direction, which are measured at 1 AU, may then be considered the result of the evolution of such coronal structures.

Taking definitely the point of view of a solar origin of magnetic structures of the type presented in this paper, it is worthed to compare in more detail the results of our analysis with the predictions of Pneuman's model. An initially ideal neutral sheet above a helmet streamer, of the type considered by Pneumann, would remain as such in the absence of dissipative effects (and thus be measured at 1 AU as a purely one dimensional configuration of antiparallel magnetic lines). The evolution into a magnetic tongue (i.e. the development of a transverse magnetic field component re-connecting the initially antiparallel magnetic lines) is in fact obtained by taking into account a finite plasma resistivity. As the resistivity of the coronal and solar wind plasma is indeed very small (Reynold numbers  $\sim 10^8$ ), the reconnecting magnetic component is correspondingly very small, i.e. the magnetic configurations which are obtained are still very close to one-dimensional neutral sheets. To give numbers, for reasonable boundary values

of magnetic field and plasma parameters at the corona, Pneuman's solution corresponds to a transverse field, at 1 AU, of  $3 \times 10^{-12}$  gauss, against a radial field of  $5 \times 10^{-5}$  gauss (which is of the order of the fields measured at 1 AU).

Clearly, these types of steady state solutions do not correspond to the structures we have analyzed in Sect. 2 as, for each of these (going to the plane of maximum variance), we have found that the component transverse to the reversing one is at least of the order of  $0.5 \div 1 \gamma$  (see the cases of days 22, 26) and more in the other cases considered.

The conclusion that we draw from such comparison is that, if we want to relate structures of the type observed here, to the evolution of an ideal neutral sheet formed in the solar corona, we must invoke a mechanism much faster than ordinary resistive diffusion and thus capable of leading to the development of an appreciable transverse component, by the time the structure has been convected from the Sun to 1 AU.

We must add that the idea of relating structures involving sharp magnetic field rotations at 1 AU, with the evolution of neutral sheets from the corona, appears, in particular, to be very natural, for events like those of days 22, 26 and 44, among those discussed in Sect. 2. These cases, which are characterized by the presence of a significant transverse component just in the reversal region, are in fact certainly more closely related to reconnected neutral sheets, than other cases involving more continuous variations, over longer scales, of both the reversing and the transverse components.

As a second point, we must comment on some very recent theoretical work (Lemaire and Burlaga, 1976) on the structure of interplanetary boundary layers. In such work, steady state solutions of the Vlasov equation have been obtained, representing magnetic



variations corresponding to those observed in some interplanetary discontinuities. Upon varying boundary conditions, at the two sides of the layer, a variety of structures are indeed obtained, including, or not, variations of magnetic field intensity and/or magnetic field rotation.

We remark, first of all, that these solutions have typical thicknesses of the order of the ion Larmor radius, whereas our events, as we will see, involve, in all cases, much longer length scales. Furthermore, solutions with a magnetic rotation much more localized than the depression have not been obtained.

A second point, in line with our way of reasoning, is that, even when explicit steady state solutions are obtained, the problem of the stability of such solutions should be considered. To make a good example, one can find a self consistent equilibrium solution of the Vlasov equation (Harris, 1964) which, as far as the magnetic field behaviour is concerned, represents a purely one dimensional reversing magnetic configuration, i.e. an ideal neutral sheet. However, a kinetic stability analysis (Dobrowolny, 1968; Galeev, 1977) reveals that this configuration is unstable and the equilibrium current sheet tends in fact to break into a periodic structure of current loops.

Clearly therefore, the relevance of a given equilibrium solution, to a configuration observed in space, is related to the fact of being able to decide if this solution is stable or not and, in the unstable cases, to decide, in relation to the growth rate, if one should or should not see the results of the instability evolution on the data.

#### 4. EVIDENCE FOR TEARING MODE INSTABILITY.

As seen in the previous section, given an ideal neutral sheet on the solar corona, ordinary resistive diffusion is not a mechanism strong enough to lead to the development of a transverse reconnecting component, of the magnitude shown by the observations, by the time this structure has reached 1 AU.

As alternative candidates for the development of an appreciable transverse component in the region of reversal of the original one, we consider now tearing mode instabilities.

Such instabilities of one dimensional current sheets, first pointed out by Dungey (1958), lead to the coalescence of the current sheet into pinches or to the evolution of the initial magnetic configuration into loops.

It could be remarked that our observations are not directly indicative of loops. However, in the presence of a looped magnetic structure, the successive loops could only be revealed when the relative motion between the magnetic structure (convected by the solar wind) and the spacecraft, occurs almost along the axis of the structure itself (the  $\underline{V}_1$  direction, corresponding to our minimum variance analysis). Crossing at other angles, would show up in the data in the form of magnetic dips with rotation of the magnetic vector, like in the events which have been analyzed here. Thus, it is legitimate to ask if the observed structures may be the non linear result of a tearing instability.

It must be pointed out that we are not claiming that this is the only possibility leading to structures of the type observed. It is indeed conceivable that some of the two dimensional magnetic field events shown in our data are simply steady state structures having already this form in the corona and then convec-

ted in the wind. The hypothesis of a tearing mode origin is, however, sufficiently interesting to deserve testing on the data and, on the other hand, as already commented in Sect. 3, appears particularly reasonable for those of the events which resemble almost one dimensional and reconnected neutral sheets.

More precisely then, referring again to our plane ( $V_1, V_2$ ) of maximum variation, we ask ourselves if the observed transverse component  $V_2$  (which is present at the zero of the main component  $V_1$ ), could be the reconnecting component obtained as a result of a tearing mode instability on an originally ideal neutral sheet being formed in the lower corona (and essentially represented by the variation of the  $V_1$  component).

The above tentative hypothesis on the origin of the transverse component, can be checked using the results of the data analysis, in a way similar to that used in a previous work on the structure of sector boundaries in the solar wind (Bavassano et al., 1976).

The linear stability of magnetic neutral sheets has been studied, both in the framework of resistive magnetohydrodynamics (Furth et al., 1963), and from the point of view of Vlasov theory (Dobrowolny, 1968; Schindler and Soop, 1968; Galeev, 1977).

The growth rate  $\gamma$  of the resistive instability is found to be given by

$$\gamma \sim \frac{1}{\tau_R} (k \lambda)^{-\frac{2}{5}} S^{\frac{2}{5}} \quad (1)$$

where

$$S = \frac{\tau_R}{\tau_H} \quad (2)$$

and

$$\tau_R = \frac{4\pi\lambda^2}{\eta}, \quad \tau_H = \frac{\lambda(4\pi\rho)^{1/2}}{B_0} \quad (3)$$

are the resistive diffusion time and the Alfvénic time respectively,

$\eta$  being the plasma resistivity,  $\rho$  the plasma density,  $B_0$  the constant magnetic field value outside the transition and  $\lambda$  the thickness of the current sheet. Finally,  $k$  is the wave number of the periodic looped configuration, resulting from the instability, along the sheet axis.

It is seen from (1) that the growth time  $\gamma^{-1}$  is shorter than the resistive diffusion time  $\tau_R$  and longer than the Alfvénic time  $\tau_H$ , thus indicating that this instability is a stronger mechanism than ordinary resistive diffusion, to cause reconnection of initially antiparallel magnetic lines.

From numerical work on the resistive tearing modes (Cross and Van Hoven, 1971), it is further found that the maximum growth rate of the modes, is approximately given by

$$\gamma \sim 3.4 (S)^{0.57} \frac{1}{\tau_R} \quad (4)$$

The wavelengths of maximum growth rate scales like :  $k \lambda \sim S^{-0.42}$ . For typical solar wind parameters and scale length of the observed structures (see Table 1) one obtains  $S \sim 10^9$  and, correspondingly  $k^{-1} \sim 10^4 \lambda$  so that the loops resulting from the instability are likely to be enormously distended along the axis of the current sheets. This is in turn a good reason why one should not expect to see a looped structure from the magnetic data.

The growth rate of the collisionless instability is found to be given by (Dobrowolny, 1968; Galeev, 1977)

$$\gamma = \sum_{j=i,e} \gamma_j = 2\sqrt{\pi} \sum_j \frac{v_j}{\lambda} \left( \frac{a_{j1}}{\lambda} \right)^{3/2} \left( 1 + \frac{T_i}{T_e} \right) \quad (5)$$

where  $j = i, e$  for ions and electrons respectively. Here  $v_j$  denotes the particle thermal velocity and  $a_{j1}$  the particle Larmor radius

calculated from the value of the  $V_1$  (reversing) component of the magnetic field outside the transition.

The dissipative mechanism responsible for the change in magnetic topology induced by this instability is given by Landau resonance between the excited waves and those particles (ions and electrons) which are trapped in the region of quasi-zero magnetic field (Dobrowolny, 1968). Correspondingly, we have in (5) two different contributions, one from the ions and one from the electrons, to the growth rate.

Non linear theories of the tearing mode instabilities (Cross and Van Hoven, 1973; Galeev, 1977) are on the other hand not so much developed (especially in the kinetic case) as to give a precise prediction on their non linear states and the typical times necessary to reach them.

In order for these instabilities (or any other instability) to be significant for a given structure, observed in the solar wind, we must impose that the typical time for instability development must be shorter than the convection time, from the corona to the point of observation of the given structure, i.e., in order of magnitude,

$$\gamma R / V_0 > 1 \quad (6)$$

where  $R$  is the radial distance from the Sun at which the configuration is observed (reported in Table 1 for the various cases), and  $V_0$  an average velocity with which the observed structure has been convected. In the following, in the absence of a clear indication from non linear theory, we will use for  $\gamma$  the linear growth rate of the instability under discussion (having in mind that this may be an overestimate) and, for  $V_0$ , using plasma data from the plasma experiment on HELIOS 1, (Rosenbauer et al., 1977) we will take the solar wind

velocity value at the times of observation of the considered structures (these are also listed in Table 1).

As the growth rates (4) and (5), of both resistive and collisionless tearing modes, increase with decreasing scale length of the equilibrium magnetic transition, using (4) and (5) into the convective criterion (6), leads to the determination of upper limiting values for the thickness of the original neutral sheet, i.e.

$$\lambda < L_{1,2j} \quad (7)$$

where

$$L_1 = (V_A R / 0.3 v_o)^{7/10} (10^4 T_{ev}^2 \beta^{-1/2})^{-3/10} \quad (8)$$

is the critical value obtained with reference to resistive tearing modes and

$$L_{2j} = \left[ \frac{1}{\sqrt{\pi}} \frac{v_j}{V_o} R \left( 1 + \frac{T_i}{T_e} \right) \right]^{2/5} a_{j1}^{3/5} \quad (9)$$

the analogous value referring to the collisionless instability driven by particles of species  $j$ .

In (8),  $V_A$  is the Alfvén velocity,  $\beta = 4\pi n(T_i + T_e)/B^2$ ,  $T_{ev}$  is the electron temperature in eV and  $a_{j1}$  the particle Larmor radius corresponding to the value of the  $V_1$  magnetic component outside the transition. Concerning the occurrence of the collisionless instability, we must add a further observation. The theory leading to the growth rate (5) is based on a purely one dimensional magnetic equilibrium. On the other hand, at least in some of the cases shown in Sect. 2 (see Figs. 4, 5, 6), the minimum variance analysis has indicated the presence of a non zero magnetic component in the direction ( $V_3$ ), normal to the plane of

maximum variation. As discussed by Biskamp et al. (1970), the further condition

$$\frac{\gamma}{\Omega_{c3}} > 1 \quad (10)$$

(where  $\Omega_{c3}$ , is the cyclotron frequency corresponding to the value of the normal component), is necessary if the result (5) of the instability theory without such component, has to hold. In the opposite case, as the particle orbits are strongly modified by such normal component, we can only say that the one dimensional theory is no more valid. Indeed, this is one equilibrium whose stability has not been investigated at the kinetic level, so that we cannot say if there is or there is not an instability.

Condition (10) gives, upon using (5),

$$\lambda < L_{3j} \quad (11)$$

where the new critical lengths  $L_{3j}$  are given by

$$L_{3j} = \left[ 2\sqrt{\pi} \cdot \left( 1 + \frac{T_i}{T_e} \right) a_{j3} \right]^{2/5} a_{jx}^{3/5} \quad (12)$$

$a_{j3}$  being the particle Larmor radius in the normal magnetic field

It is  $L_{3e}/L_{3i} \sim 2.3 \times 10^{-2} \left( \frac{T_e}{T_i} \right)^{1/2}$  and, from (9),  $L_{2e}/L_{2i} \sim 0.47 \left( \frac{T_e}{T_i} \right)^{1/2}$  so that (7) and (11) are less stringent for the ion than for the electron collisionless tearing mode.

As can be seen from formulas (8), (9) and (12), the three critical lengths  $L_1$ ,  $L_{2j}$  and  $L_{3j}$  can all be calculated, for each of the magnetic dips considered in Sect. 2, by using the results of our minimum variance analysis.

In addition we have used averaged values for plasma density, velo-

city and ion temperature from the proton experiment of on HELIOS 1 (Rosenbauer et al., 1977). The electron temperature has been further derived by using the experimentally observed correlation between the ratio  $T_e/T_i$  and the wind bulk flow (Montgomery 1972).

The orientations of the observed magnetic sheets, reported in Table 2, is used to obtain the wind velocity component  $V_{o2}$  normal to the sheets, i.e. in our  $\underline{V}_2$  direction (this was done assuming the bulk flow to be in the radial direction).

In turn, the values of  $V_{o2}$  (together with the time duration where the magnetic reversal occurs), give the space thickness  $\lambda$  of the current sheets.

Values of  $V_{o2}$  and  $\lambda$  are reported in Table 1. As it is seen there are cases where the wind flow is almost normal to the magnetic reversal and cases where, on the contrary, it is at a small angle with respect to the axis of the sheet.

Rather thin events on the time scale may thus in reality correspond to comparatively large space variation and viceversa. In every case considered, however, the sheet thickness  $\lambda$  is found to be much larger than the ion Larmor radius (typically  $\sim 50\div 100$  km). In the same Table 1, we have finally reported also the values obtained for the three critical lengths defined previously.

Notice that, for the normal magnetic field component  $V_3$ , to be used in (12), we have taken an average of the values resulting from the variance analysis in the region of linear variation of the reversing component  $V_1$  near its zero.

The following results may be pointed out from an examination of Table 1.

With the exception of the events of day 22 and day 44, the length  $L_{3i}$  is much smaller than the thickness  $\lambda$  of the observed



magnetic reversals. Thus, in all cases (except those of day 22 and 44) the collisionless instability seems to be ruled out as a possibility for explaining the reconnecting component ( $V_2$ ) in the observed structures. On the other hand, we cannot draw any conclusion for the events of day 22 and 44, where the two numbers calculated for  $\lambda$  and  $L_{3i}$  are about equal.

Concerning the occurrence of resistive tearing modes, we see from Table 1 that the criterium (7)  $\lambda < L_1$  is largely satisfied for the events of day 22 and 44. We think it is significant to remark that these are cases which closely resemble almost one dimensional reconnected neutral sheets, as already discussed. For a third event of this type (day 26) the two numbers for  $\lambda$  and  $L_1$  are quite close together.

An interesting feature of the events of day 22 and 26, which we have deduced from plasma data at a resolution of 40 s, supplied to us by R. Schwenn, is that a rotation of the velocity vector appears to be associated with the magnetic rotation.

This is very interesting because it corresponds, at least qualitatively, to what one expects from models of steady state reconnection and, at least qualitatively, also for a configuration resulting from the non linear development of a tearing mode.

In the case of the event of day 26, where the magnetic rotation takes place essentially in the ecliptic plane (see Table 1), the velocity rotation is also in that plane. More precisely, it is the azimuthal velocity component which rotates and its magnitude can be roughly estimated to be  $\sim 40$  km/s, i.e. of the order of the Alfvén velocity. For the event of day 22, we see from the plasma data that both the azimuthal and the latitudinal velocity angles change, so that the velocity rotation is in a plane different from the ecliptic (like the magnetic rotation, as seen from Table 1).

It should also be added that no such significant rotation is found to accompany the larger events of day 3 and 18 (consistently with our guess that these are not related to tearing modes). As for the remaining three cases, which differ from the previous ones because of the presence of an appreciable transverse component along all the transition, we find that, for the event of day 18,  $\lambda \gg L_1$ , so that this magnetic transition has certainly nothing to do with the development of a tearing mode. For the events of day 3 and 85, on the other hand, the two lengths  $\lambda$  and  $L_1$  appear to be close together.

In cases of this type we cannot draw any conclusion owing to uncertainties in the determination of both  $\lambda$  and the tearing mode critical lengths and also to the approximate character of the condition (7) we are imposing.

## 5. SUMMARY AND DISCUSSION.

Using HELIOS 1 magnetic data, we have investigated, through a minimum variance analysis, the structure of several discontinuities in the form of magnetic dips with accompanying rotation of the magnetic field vector.

From the analysis we deduce that some of the events considered resemble almost one dimensional neutral sheets with a transverse component arising around the zero of the main reversing component. In other cases the variations can be said to be more two-dimensional, with an appreciable transverse component always present during all the magnetic depression.

We have tested the theoretical idea that, at least in some cases, the transverse magnetic component can be the result of the non linear development of a tearing mode instability on an initially ideal neutral sheet formed at the solar corona. The idea seems indeed to be particularly appropriate for the almost one dimensional events mentioned above.

For two of such events (day 22 and day 44, see Figs. 2 and 3), we find in fact consistency with the idea of origin from a resistive tearing mode and, for a third one of the same type (day 26), marginal consistency. Besides, from the plasma data available, for the events of day 22 and 26 there is evidence of a rotation of the velocity vector associated with a magnetic field rotation. This is also qualitatively expected for a configuration resulting from tearing modes and thus supports our idea.

On the other hand, a clearly "two-dimensional" transition, like that of day 18 (see Fig. 1), involving a continuous magnetic field rotation throughout the magnetic dip, has been found to have nothing to do with tearing modes. In other similar cases, we cannot

reach firm conclusions as the lengths we are comparing turn out to be quite close and, on the other hand, there are uncertainties in the data used.

In conclusion, the idea of a magnetic reconnection process (for example a tearing mode) having generated structures of the type considered, is strongly suggested by our analysis for some of the cases treated. It therefore appears of interest, in order to gain more definite conclusions, to pursue further this idea on the basis of a greater number of events. Besides, high resolution plasma data should also be analyzed, in order to understand plasma behaviour through these transitions and, in particular, to study qualitatively the changes and rotations of velocity flow associated with such magnetic discontinuities.

#### ACKNOWLEDGEMENTS

The authors thank Dr. H. Rosenbauer and Dr. R. Schwenn for having supplied plasma data for the events considered here.

## REFERENCES

- Bavassano B., Dobrowolny M. and Mariani F.: 1976, *J. Geophys. Res.* 81, 1.
- Burlaga L.F.: 1971, *Space Sci. Rev.* 12, 600.
- Burlaga L.F.: 1971, *J. Geophys. Res.* 76, 4360.
- Burlaga L.F. and Ness N.F.: 1969, *Solar Phys.* 9, 467.
- Burlaga L.F., Lemaire J.F. and Turner J.M.: 1976, GSFC Report X-692-76-168.
- Burlaga L.F. and Scudder J.O.: 1974, *Astrophys. J.* 191, L149.
- Cross M.A. and Van Hoven G.: 1971, *Phys. Rev.* A4, 2347.
- Dobrowolny M.: 1968, *Nuovo Cimento* 55b, 427.
- Dungey J.W.: 1958, "Cosmic Electrodynamics" p. 98, Cambridge Un. Press, New York.
- Furth H.P., Killeen J. and Rosenbluth M.N.: 1963, *Phys. of Fluids* 6, 459.
- Galeev A.A. and Zeleny L.M.: 1976, *Sov. Phys. JETP* 42, 450.
- Harris E.G.: 1962, *Nuovo Cimento* 23, 115.
- Lemaire J. and Burlaga L.F.: 1976, *Astrophys. and Space Sci.* 45, 303.
- Mariani F., Burlaga L.F., Ness N.F., Bavassano B., Villante U., Rosenbauer H. and Schwenn R.: 1978, to be published in JGR.
- Mariani F., Bavassano B., Villante U. and Ness N.F.: 1973, *J. Geophys. Res.* 78, 8011.
- Martin R.N., Belcher J.W. and Lazarus A.J.: 1973, *J. Geophys. Res.* 78, 3653.
- Montgomery M.D.: 1972, in "Solar Wind", NASA SP-308, p. 208.
- Parker E.N.: 1977, *Astrophys. J. Suppl. No. 77*, 8.
- Pneumann G.W.: 1972, *Solar Phys.* 23, 223.
- Rosenbauer H., Schwenn R., Marsch E., Meyer B., Miggenrieder H., Montgomery M.D., Mülhäuser K.H., Pilipp W., Voges W. and Zink S.M.: 1977, *J. Geophys. Res.* 42, 561.

- Scearce C., Cantarano S., Ness N., Mariani F., Terenzi R., Burlaga L.: 1975, GSFC Report X-692-75-112.
- Schindler K.M. and Soop M.: 1968, Phys. of Fluids 11, 1192.
- Siscoe G.L., Davis L.Jr., Coleman P.J.Jr., Smith E.J. and Jones D.E.: 1968, J. Geophys. Res. 73, 61.
- Sonnerupp B.V. and Cahill L.J.: 1967, J. Geophys. Res. 72, 171.
- Tsurutani B.T. and Smith E.J.: 1971, EOS Trans. AGU 56, 1055.
- Turner J.M., Burlaga L.F., Ness N.F. and Lemaire J.F.: 1976, GSFC Report X-692-76-90.
- Van Hoven G. and Cross M.A.: 1973, Phys. Rev. A4, 1347.

TABLE 1 : OBSERVED CURRENT SHEETS AND CHARACTERISTIC LENGTHS

Time of occurrence		Eliocentric distance (AU)	$V_o$ (km/s)	$V_{o2}$ (km/s)	$\lambda, 10^3$ km	$L_1, 10^3$ km	$L_{2i}, 10^3$ km	$L_{3i}, 10^3$ km
Year	Day Hour							
1975	3 14h, 2'	0.938	510	88	2.7	2.0	15.5	0.48
1975	18 13h, 45'	0.859	500	137	19.2	3.2	11.2	0.48
1975	22 21h, 56'	0.829	360	42	0.5	3.1	10.8	0.68
1975	26 1h, 21'	0.805	540	523	2.6	2.1	12.7	0.75
1975	44 20h, 22'	0.622	690	643	0.3	2.5	7.9	0.27
1975	85 8h, 11'	0.388	360	61	1.3	1.2	6.4	0.26

TABLE 2  
EIGENVALUE RATIOS AND EIGENVECTORS FROM THE VARIANCE ANALYSIS.

DAY	$E_2/E_1$	$E_3/E_1$	$E_3/E_2$	$V_{-1}$			$V_{-2}$			$V_{-3}$			$(\Delta t)$	N
				x	y	z	x	y	z	x	y	z		
3	0.009	0.004	0.403	0.97	0.15	0.20	-0.17	0.98	0.12	-0.18	-0.15	0.97	14 <sup>h</sup> 0' 45" - 14 <sup>h</sup> 2' 45"	120
18	0.056	0.012	0.215	0.90	0.12	0.43	-0.27	0.90	0.33	-0.35	-0.42	0.84	13 <sup>h</sup> 42' 58" - 13 <sup>h</sup> 48' 12"	314
22	0.053	0.005	0.098	0.75	0.63	0.19	-0.12	-0.16	0.98	0.65	-0.76	-0.04	21 <sup>h</sup> 56' 4" - 21 <sup>h</sup> 56' 22"	96
26	0.017	0.011	0.604	-0.17	0.96	0.23	0.97	0.12	0.22	0.18	0.26	-0.95	1 <sup>h</sup> 21' 35" - 1 <sup>h</sup> 22' 15"	213
44	0.021	0.005	0.220	0.35	0.64	0.69	0.93	-0.31	-0.18	0.10	0.70	-0.71	20 <sup>h</sup> 22' 30" - 20 <sup>h</sup> 22' 57"	144
85	0.064	0.005	0.078	0.76	-0.60	0.25	0.17	0.55	0.82	-0.63	-0.58	0.52	8 <sup>h</sup> 10' 20" - 8 <sup>h</sup> 12' 40"	93



## FIGURE CAPTIONS

- Fig. 1. Magnetic field intensity and direction for the day 18 event. Theta is the inclination with respect to the ecliptic plane (positive in the north direction, negative in the south direction), and Phi is the azimuth in the ecliptic plane ( $0^\circ$  toward the Sun and rotated anticlockwise). The plot shows 1 s averages of the full resolution data.
- Fig. 2. Same as Figure 1, for the day 22 event. The plot shows the full resolution data.
- Fig. 3. Same as Figure 1, for the day 44 event. The plot shows the full resolution data. The small fluctuations are mainly due to a residual spin modulation.
- Fig. 4. Magnetic field components in the eigenvectors reference for the day 18 event.  $V_1$  component is along  $\underline{V}_1$  direction,  $V_2$  component along  $\underline{V}_2$  direction,  $V_3$  component along  $\underline{V}_3$  direction,  $\underline{V}_1$ ,  $\underline{V}_2$  and  $\underline{V}_3$  being the eigenvectors obtained from the variance analysis.
- Fig. 5. Same as Figure 4, for the day 22 event.
- Fig. 6. Same as Figure 4, for the day 44 event.
- Fig. 7. Variation across the sheet of the magnetic field projection on the plane of maximum variance for the 6 events listed in Table 1. Each diagram is obtained by plotting in temporal sequence the magnetic field projection on the plane  $(\underline{V}_1, \underline{V}_2)$ , each vector having its origin on the tip of the preceding vector. Dots visualize the vectors sequence, A being the origin of the first vector and B the end of the last vector in the indicated time interval.



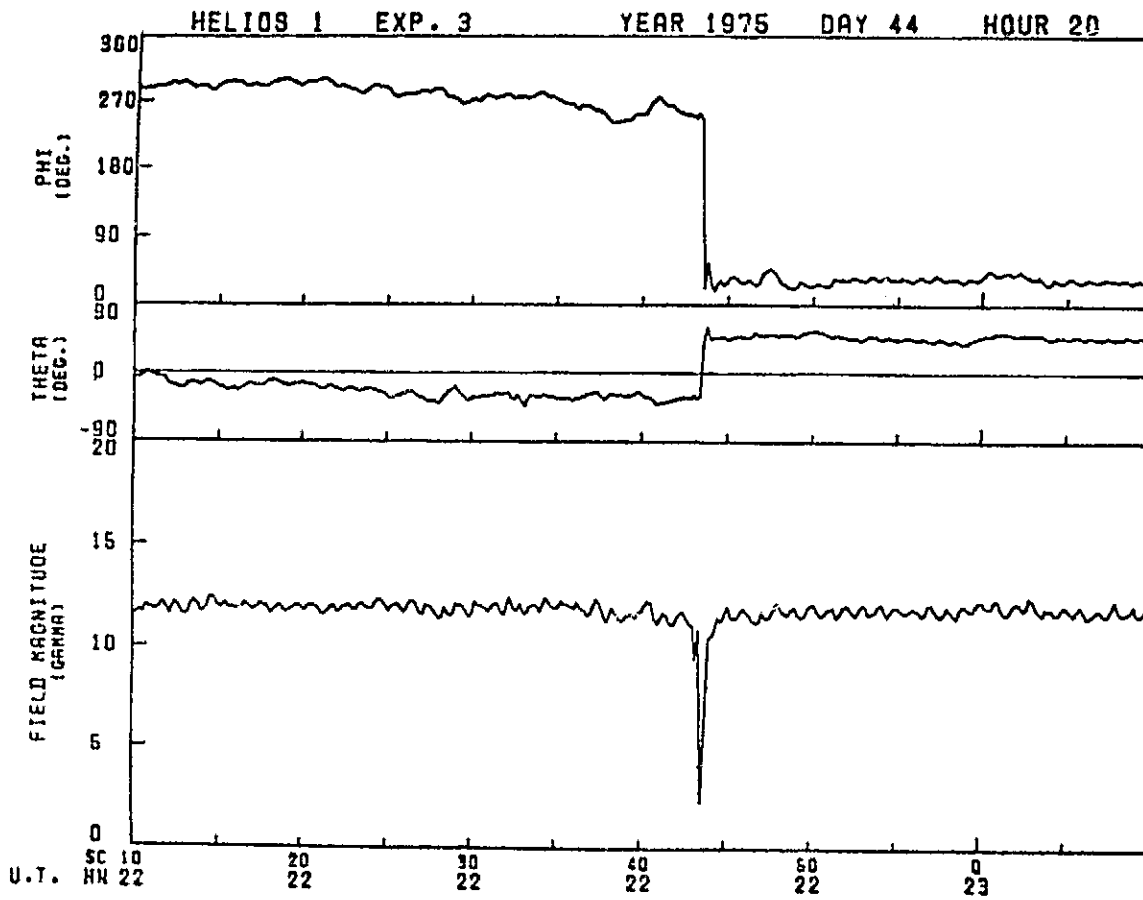


FIG. 3

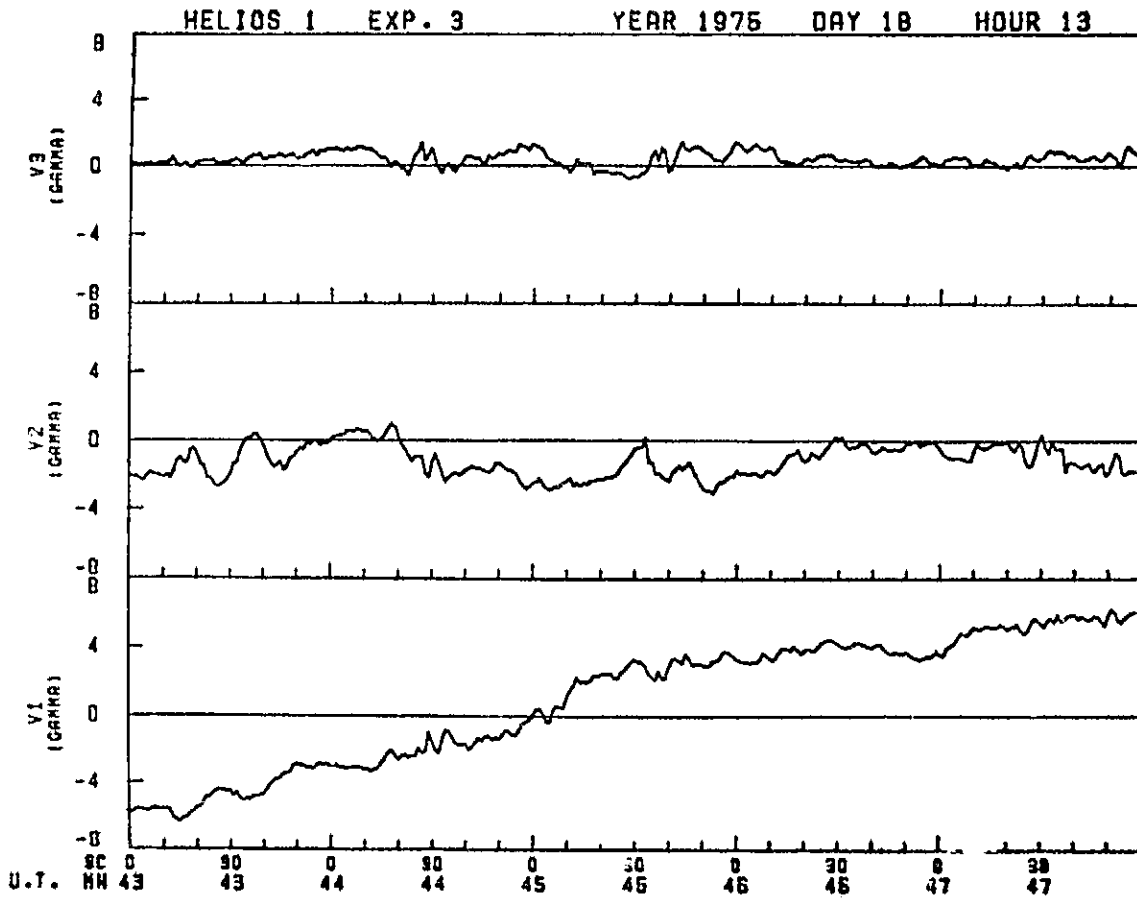


FIG. 4

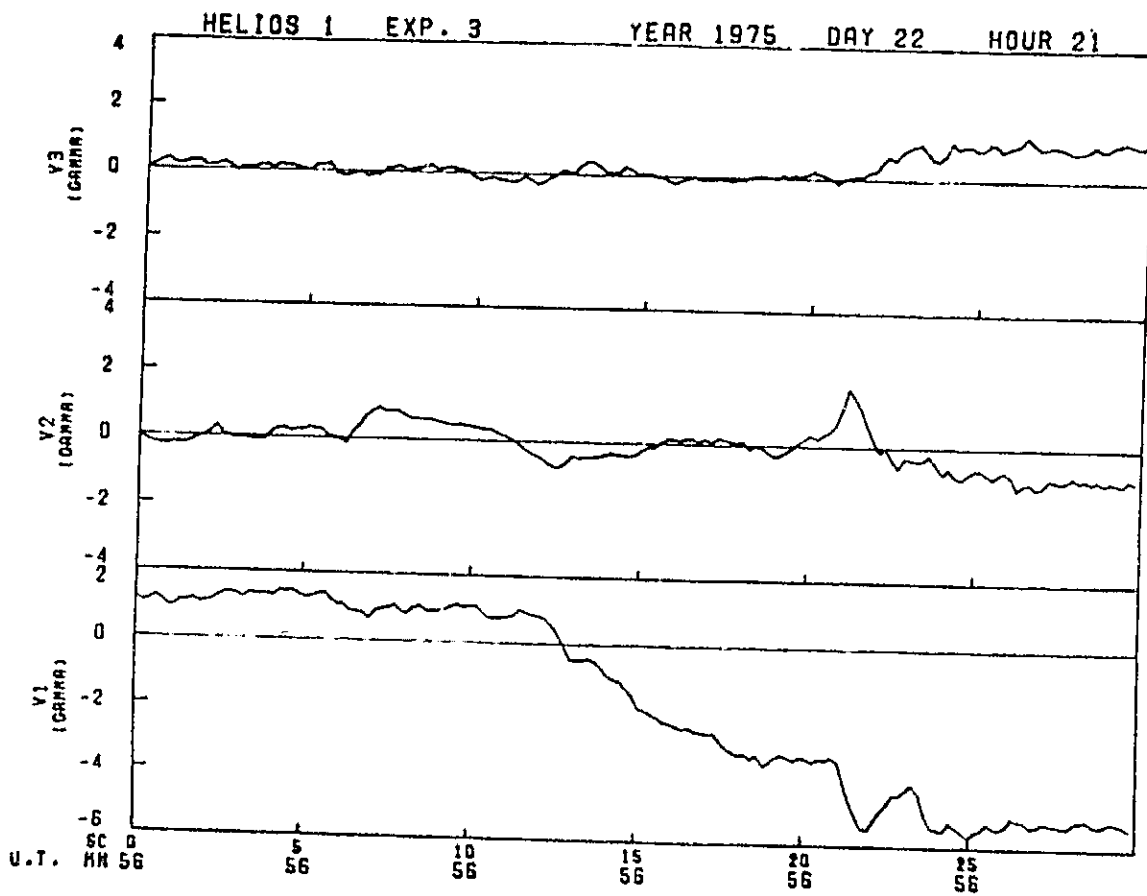


FIG. 5

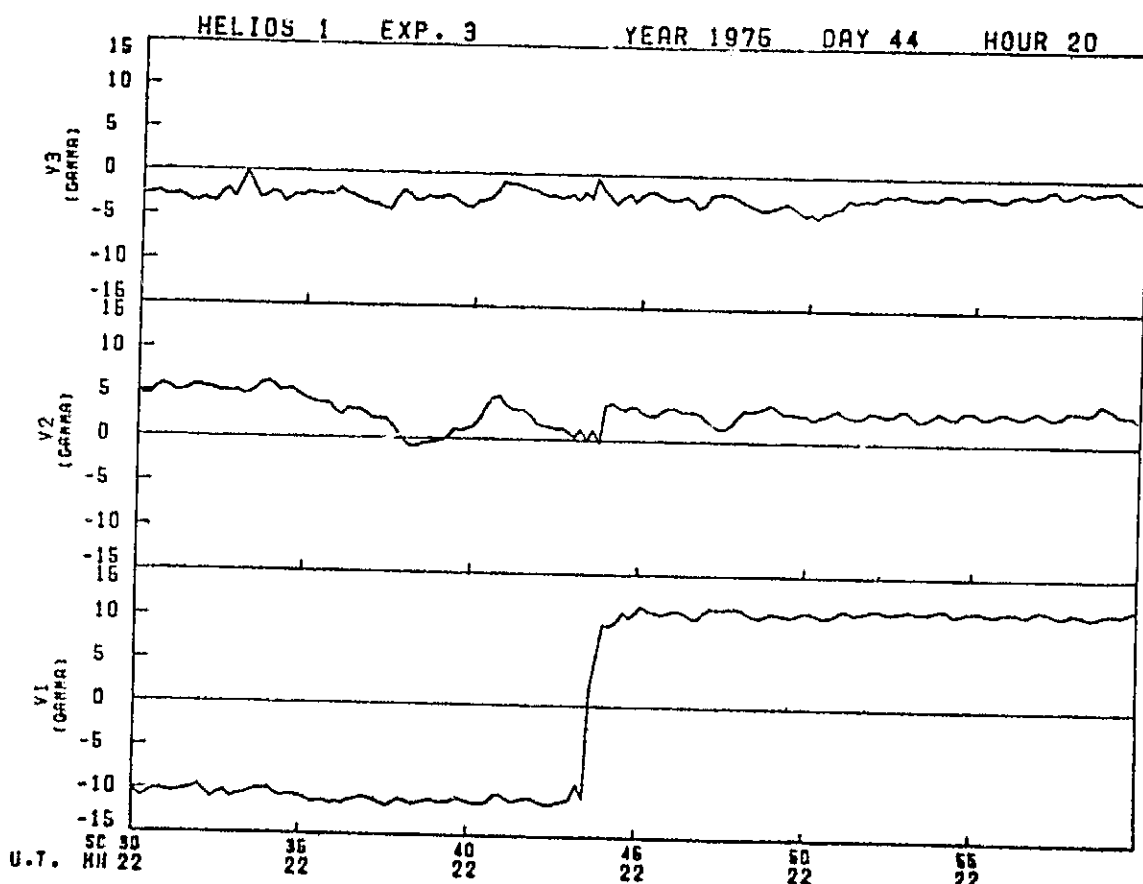


FIG. 6

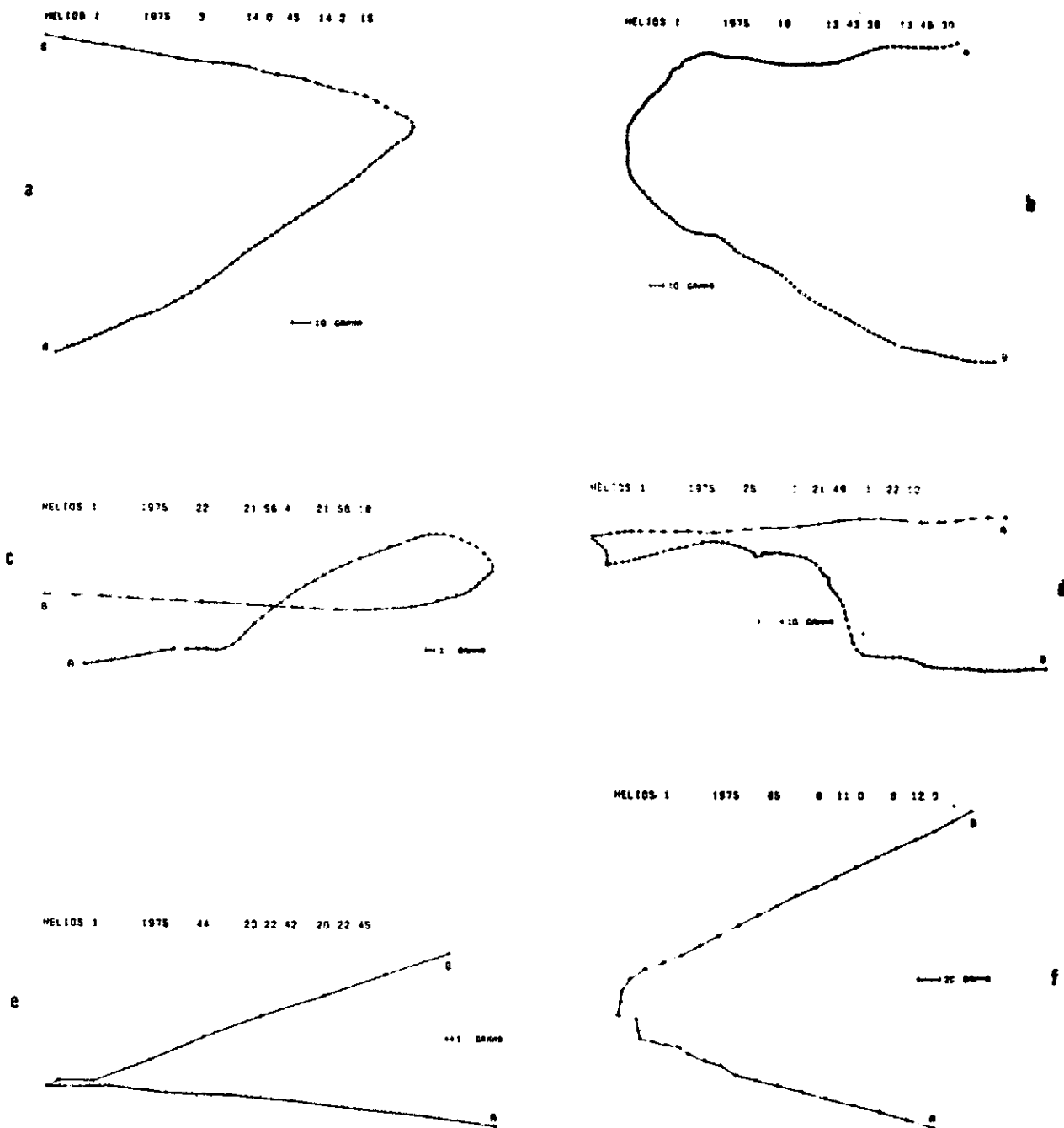


FIG. 7